


Shewanella khirikhana sp. nov. – a shrimp pathogen isolated from a cultivation pond exhibiting early mortality syndrome

Anuphap Prachumwat,^{1,2}  Piyanuch Wechprasit,^{2,3} Jiraporn Srisala,¹ Ruttanaporn Kriangsaksri,^{2,3} Timothy W. Flegel,^{2,4} Siripong Thitamadee^{2,3} and Kallaya Sritunyalucksana^{1*} 

¹Aquatic Animal Health Research Team, Integrative Aquaculture Biotechnology Research Group, National Center for Genetic Engineering and Biotechnology (BIOTEC), National Science and Technology Development Agency (NSTDA), Pathum Thani, Thailand.

²Center of Excellence for Shrimp Molecular Biology and Biotechnology (Centex Shrimp), Faculty of Science, Mahidol University, Bangkok, Thailand.

³Department of Biotechnology, Faculty of Science, Mahidol University, Bangkok, Thailand.

⁴National Center for Genetic Engineering and Biotechnology (BIOTEC), National Science and Technology Development Agency (NSTDA), Pathum Thani, Thailand.

Summary

Early mortality syndrome (EMS) in cultivated shrimp is of complex aetiology. One of the causes is acute hepatopancreatic necrosis disease (AHPND) caused by unique *Vibrio* isolates that carry two *Pir*^{VP} toxin genes, but other causes of EMS remain mostly unexplained. Here, we describe the discovery of a *Shewanella* isolate TH2012^T from an EMS/AHPND outbreak pond and demonstrate its virulence for shrimp (the mean lethal concentration of 10⁵ colony-forming units per millilitre by immersion challenge) accompanied by distinctive histopathology, particularly of the ventral nerve cord and lymphoid organ but

also including the digestive tract. On the basis of its complete genome sequence, multilocus phylogenetic trees, digital DNA–DNA hybridization analysis and differential phenotypic characteristics, we propose that *Shewanella* isolate TH2012^T represents a novel species, separated sufficiently from the type strains *S. listorisediminis* and *S. amazonensis* to justify naming it *Shewanella khirikhana* sp. nov. Analysis of the TH2012^T genome revealed no homologues of the *Pir*^{VP} toxin genes but revealed a number of other potential virulence factors. It constitutes the first *Shewanella* isolate reported to be pathogenic to shrimp.

Introduction

The history and current status of early mortality syndrome (EMS) and its component acute hepatopancreatic necrosis disease (AHPND) have recently been reviewed (Thitamadee *et al.*, 2016; Prachumwat *et al.*, 2019). Briefly, outbreaks began in China around 2009 and spread to several countries in Asia (Thitamadee *et al.*, 2016; Prachumwat *et al.*, 2019) before reaching Mexico (Nunan *et al.*, 2014) in 2013. More recently, outbreaks have been reported from the Philippines (De La Peña *et al.*, 2015), Australia (World Organization for Animal Health, 2016) and the USA (Dhar *et al.*, 2018). The AHPND component of EMS is the most severe bacterial disease so far reported for cultivated shrimp and has caused massive production losses since 2009. In 2013, the cause of AHPND was reported to be unique isolates of *Vibrio parahaemolyticus* (VP_{AHPND}) that produced *Pir*^{VP} toxins A and B from genes on a conjugative plasmid called pVA (Tran *et al.*, 2013; Lee *et al.*, 2015; Sirikharin *et al.*, 2015). AHPND accounts for only a portion of the disease outbreaks that shrimp farmers collectively call early mortality syndrome (EMS) (Sanguanrut *et al.*, 2018) and so cannot be equated with EMS that shrimp farmers use to refer to any early mortality whatever the cause (Thitamadee *et al.*, 2016). Thus, all reports of putative AHPND outbreaks that arise by equating EMS with AHPND must be considered scientifically unreliable, unless they are accompanied by confirmation in the form of evidence for pathognomonic AHPND lesions, PCR detection of VP_{AHPND} or immunological detection of *Pir*^{VP} toxins A and B. At the same time, EMS outbreaks not

Received 25 August, 2019; revised 4 January, 2020; accepted 10 January, 2020.

*For correspondence. E-mail kallaya@biotec.or.th; Tel. +66 2644 8150 ext. 81851; Fax +66 2354 7344.

Microbial Biotechnology (2020) 13(3), 781–795
doi:10.1111/1751-7915.13538

Funding Information

This work was supported by the Agricultural Research Development Agency (ARDA) (grant number 8669), Mahidol University and the National Center for Genetic Engineering and Biotechnology (BIOTEC) of the National Science and Technology Development Agency (NSTDA). PW also would like to acknowledge the support from Thailand Graduate Institute of Science and Technology Scholarship (TGIST grant number SCA-CO-2560-4497-TH).

© 2020 The Authors. *Microbial Biotechnology* published by John Wiley & Sons Ltd and Society for Applied Microbiology.

This is an open access article under the terms of the Creative Commons Attribution-NonCommercial-NoDerivs License, which permits use and distribution in any medium, provided the original work is properly cited, the use is non-commercial and no modifications or adaptations are made.

caused by AHPND remain unexplained and possible causes could include other bacterial species.

At the same time, variation in the virulence of VP_{AHPND} isolates has been reported (Joshi *et al.*, 2014; Lai *et al.*, 2015) but no basis for it has so far been clearly identified. It has been suggested that such variation may be due to other VP_{AHPND} virulence factors that may or may not be carried by the pVA plasmid (Sirikharin *et al.*, 2015; Tinwongger *et al.*, 2016; Han *et al.*, 2017). In addition, other species of *Vibrio* have been reported to carry pVA plasmids, produce Pir^{VP} toxins A and B and cause pathognomonic AHPND lesions (Kondo *et al.*, 2015; Liu *et al.*, 2015; Han *et al.*, 2017). Even more recently, archived isolates of *Vibrio campbellii* from Thailand in 2002 (named *V. harveyii* at the time of their isolation) have been reported to produce Pir^{VP} toxins A and B and to cause AHPND (Wangman *et al.*, 2018). However, before the discovery of VP_{AHPND}, it was found that some bacterial genera not previously associated with shrimp disease occurred at a higher proportion in EMS ponds than in normal ponds (Prachumwat *et al.*, 2012; FAO, 2013). Thus, after the discovery of VP_{AHPND}, it was hypothesized that non-AHPND isolates previously obtained from AHPND outbreak ponds might have the ability to potentiate the virulence of a VP_{AHPND} isolate (FAO, 2013). Results of the study revealed that the cause of mortality in some EMS ponds was unknown (Sanguanrut *et al.*, 2018), and reports on wide variation in the virulence of AHPND isolates lent some support to this 2013 hypothesis. Thus, in a continued effort to test the hypothesis, we have been screening other bacterial isolates that have been obtained from EMS/AHPND ponds. Recently, we reported the complete genome of one such Thai isolate TH2012^T with a high similarity of 16S rRNA to those of species in the genus *Shewanella* (Wechprasit *et al.*, 2019). Here, we demonstrate that TH2012^T itself is lethal to juvenile Pacific whiteleg shrimp *Penaeus (Litopenaeus) vannamei* in laboratory challenges, and we reveal by full genome analysis that it is a new species of the genus *Shewanella* with a number of potential virulence factor genes.

Results

Organism information, genome, taxonomic classification and phenotypic features

Bacterial isolate TH2012^T was obtained together with *V. parahaemolyticus* AHPND (VP_{AHPND}) isolates 3HP and 5HP (Joshi *et al.*, 2014) from the hepatopancreas of moribund shrimp specimens obtained from a shrimp pond experiencing an EMS/AHPND outbreak. TH2012^T was initially identified tentatively based on the very high sequence identity of a 762-nucleotide 16S rRNA PCR amplicon to matching sequences from species in the

genus *Shewanella*. The complete genome sequence and genomic annotation of TH2012^T have been previously described (see Supporting information) (Wechprasit *et al.*, 2019). Details of its taxonomic classification and phenotypic features are described below.

Phylogenetic analysis. A neighbour-joining tree constructed from the concatenated multiple sequence alignments of 16S rRNA, *atpA*, *mreB* and *rpoA* genes revealed that TH2012^T resided in a clade (bootstrap re-sampling value 100%) together with other two *Shewanella* species (three strains shown in Fig. 1). The tree placed TH2012^T as a sister taxon of a subclade containing *S. litorisediminis* SMK1-12^T and TBRC 5001 and *S. amazonensis* SB2B^T (bootstrap 100%). Similarly, the placement of TH2012^T as a sister taxon with a subclade containing SMK1-12^T, TBRC 5001 and SB2B^T was also recovered by all of the other three algorithms (the minimum evolution, maximum-likelihood and maximum-likelihood algorithms; Fig. 1). The same topology of TH2012^T and the other three strains was also observed in individual trees of *atpA*, *mreB* and *rpoA* genes (Figs S3, S4 and S5). However, different topologies of these four strains were observed in trees of 16S rRNA genes (Figs S1 and S2). All trees of 16S rRNA sequences revealed that TH2012^T was most closely linked to the type strain of *S. amazonensis* SB2B^T and then clustered with the type strain of *S. litorisediminis* SMK1-12^T. Among these 16S rRNA trees, TBRC 5001 was clustered with TH2012^T or *S. amazonensis* SB2B^T (depending on algorithms) but with lower bootstrap values. Our phylogenetic tree analysis further suggested that TH2012^T and other two isolates with partial 16S rRNA sequences (*S. sp.* AK55 and *S. litorisediminis* LV 5) might be representatives of a single species (Fig. S2). Nucleotide identities of TH2012^T to homologous sequences in the other strains were 98.4–100% for 16S rRNA and 91–97% for *atpA*, *mreB* and *rpoA* genes (Table S2).

DNA–DNA relatedness. Using complete genomes of TH2012^T (Wechprasit *et al.*, 2019) and *S. amazonensis* SB2B^T to calculate dDDH similarities (see Experimental Procedures), it was found that the dDDH value was 25.2% (model 95% C.I. 22.9–27.7%). This value suggested that TH2012^T and SB2B^T were isolates of different species based on the recommendation that an dDDH > 70% should be obtained for isolates belonging to the same species (Meier-Kolthoff *et al.*, 2013). The genomic G + C contents of TH2012^T and SB2B^T were 54.80% and 53.58% respectively. This difference in genomic G + C content of 1.22% also indicates that TH2012^T and SB2B^T are different species. Furthermore,

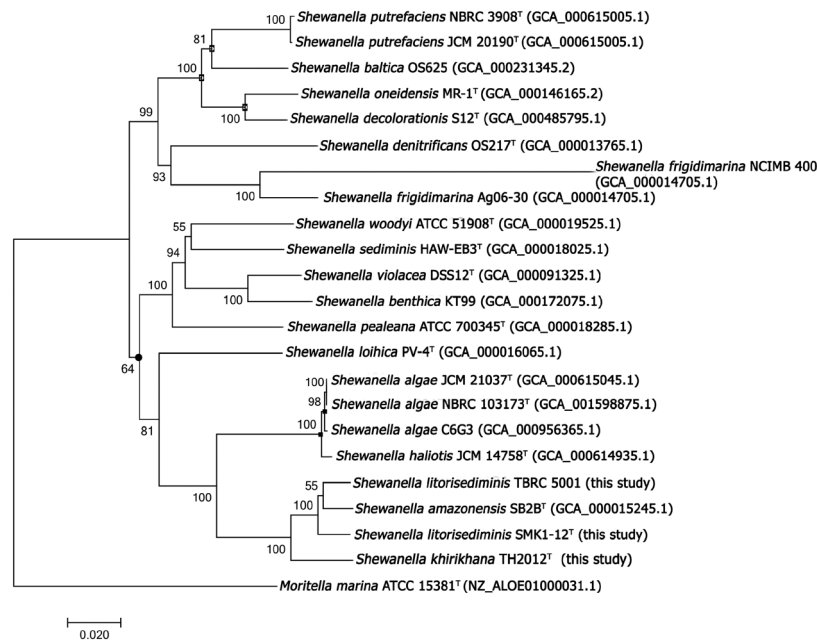


Fig. 1. Phylogenetic positions of *S. khirikhana* TH2012^T and other *Shewanella* species. The neighbour-joining phylogenetic tree with Jukes–Cantor distance was based on 4290 aligned positions of concatenated 16S rDNA, *atpA*, *mreB* and *rpoA* gene sequences. *Moritella marina* ATCC 15381 was used as an outgroup. Bootstrap values (expressed as percentages of 1000 replications) are shown at branching points. Most of the nodes were also recovered in the trees generated with the minimum evolution (Jukes–Cantor distance), maximum-likelihood (Jukes–Cantor distance) and maximum parsimonious algorithms based on the same set of sequences, except those with *Filled circles*, *Opened squares* or *Filled squares* that were not recovered in the trees of maximum parsimonious, maximum-likelihood, or both maximum parsimonious and maximum-likelihood algorithms respectively. The *scale bar* indicates estimated sequence divergence (substitutions per nucleotide position). Sequence accession numbers are shown in the parentheses after the species names.

the average nucleotide identity (ANI) scores between the complete genomes of TH2012^T and SB2B^T were 81.7%–81.8%. These ANI scores supported the proposal that TH2012^T and SB2B^T are different species, according to a cut-off at ANI > 95% identity for species boundary separation (Goris *et al.*, 2007).

Morphological and physiological characteristics of TH2012^T. TH2012^T cells are free-living, Gram-negative, straight motile rods, and their colonies on TSA + 1.5% NaCl are yellowish in colour, translucent, circular, smooth and convex with entire edges, but with no evidence of spore formation (Figs S6 and S7). Cells from broth culture measured $0.58 \pm 0.05 \times 2.02 \pm 0.38 \mu\text{m}$ ($n = 50$) in Gram-stained smears (Fig. S6B). We tested various parameters (temperatures, pH and % NaCl) on TH2012^T growth (see Supporting information) as it has been cultured in TSB supplemented by 1.5% (w/v) NaCl at 30°C in our laboratory. We found that TH2012^T could grow at temperatures 25–37°C, with supplementation of 0.5–5% (w/v) NaCl (0% NaCl was not tested), and over a pH range of 6.5–9.5, but could not grow at 4 and 42°C, with 6–8% (w/v) NaCl or at pH of 6. Since TSB already contained 0.5% NaCl, TH2012^T could grow in

supplementation with 0–5% NaCl, resulted in medium finally containing 0.5–5.5% (w/v) NaCl. Its optimal growth occurred at 30°C, pH 7–7.5 and 1.5–2% (w/v) NaCl (i.e. TSB supplemented 1–1.5% NaCl), and this constituted our routine laboratory culture conditions (Table S5, Figs S8 and S9). It died when stored at 4°C, so refrigerated storage is not recommended. TH2012^T produced H₂S, showed oxidase activity and could reduce nitrate to nitrite but did not ferment glucose and citrate and did not show ornithine decarboxylase activity. In addition, it could hydrolyse Tween 20, gelatin and casein but not urea. *S. amazonensis* SB2B^T (= ATCC 700329^T) also had similar characteristics to TH2012^T for the above investigated features, but lacked information on urease activity and gave conflicting reports on ability to ferment D-glucose and citrate (Venkateswaran *et al.*, 1998; Lee and Yoon, 2012). *S. litorisediminis* SMK1-12^T (= KCTC 23961^T) had similar features as TH2012^T and SB2B^T but was reported as non-motile with capability to ferment D-glucose (Lee and Yoon, 2012). However, we found that KCTC 23961^T (= SMK1-12^T) could not ferment D-glucose and did not show ornithine decarboxylase activity. The full phenotypic characteristics of TH2012^T in comparison with SMK1-12^T and SB2B^T are given in Table 1. TH2012^T showed

exponential growth from the end of the first to the fourth hours of liquid culture with OD600 increasing from 0.1 to 2.5, respectively, and with viable cell counts of 10^7 to 10^9 CFU ml⁻¹ at the end of the second and fourth hours respectively (Figs S10 and S11).

TH2012^T satisfies Koch's postulates as a potential shrimp pathogen

In shrimp immersion challenge tests with TH2012^T at 10^4 to 10^6 CFU ml⁻¹, mortality was first observed at 48 hpi and reached 100% by 72 hpi at all concentrations of TH2012^T except 10^4 that gave 100% mortality at 84 hpi. There was no mortality within 96 hpi in the unchallenged, negative control group consisting of untreated shrimp. Thus, the mean lethal concentration (LC₅₀) for 60 h exposure to TH2012^T was estimated to be $\sim 10^5$ CFU ml⁻¹ (Fig. S12). Histological analysis was carried out with the control and test shrimp to screen for any pathognomonic histopathology (see below).

Table 1. Differential phenotypic characteristics of *Shewanella khirikhana* TH2012^T, *S. litoreddiminis* SMK1-12^T (= KCTC 23961^T) and *S. amazonensis* SB2B^T (= ATCC 700329^T).

Characteristics	<i>Shewanella</i>		
	<i>khirikhana</i> TH2012 ^T	<i>litoreddiminis</i> SMK1-12 ^T ^a	<i>amazonensis</i> SB2B ^T ^b
Colony pigment colour	Yellowish	Yellowish	Pinkish
Gram staining	–	–	–
Motility	+	–	+
Shape	Rod	Rod	Rod
Ornithine decarboxylase	nd/+ ^c	–	–
H ₂ S production	+	+	+
Oxidase test	+	+	+
Reduction nitrate to nitrite	+	+	+
Urea hydrolysis	–	–	nd
Fermentation of D-glucose	–	+/- ^c	-/+ ^d
Citrate	–	–	+/- ^d
Hydrolysis of Tween 20	+	+	+
Enzyme activity			
Caseinase	+	+/nd ^c	nd/+ ^d
Gelatinase	+	+	+

+, positive; –, negative; nd, no data.

a. Data based on both (Lee and Yoon, 2015) and this study.

b. Data based on both (Venkateswaran *et al.*, 1998) and (Lee and Yoon, 2015).

c. The conflicting data between (Lee and Yoon, 2015)/this study (KCTC 23961^T) or not determined in this study (KCTC 23961^T).

d. The conflicting data between (Venkateswaran *et al.*, 1998)/(Lee and Yoon, 2015) (ATCC 700329^T) or not reported in (Venkateswaran *et al.*, 1998); All three strains were negative for fermentation of L-arabinose ((Lee and Yoon, 2015) and this study), but TH2012^T was also negative for fermentation of D-mannitol, inositol, D-sorbitol, L-rhamnose, D-sucrose, D-melibiose and amygdalin.

To satisfy Koch's postulates, stomach and HP tissues from the replicated challenge tests above were aseptically and individually removed from moribund shrimp, homogenized and used as an inoculum in selective TSB for re-isolation of *S. khirikhana* TH2012^T. From TSB, the turbid culture broth was streaked on selective TSA, and colonies with appropriate morphology were re-streaked on fresh selective TSA. One such isolate, confirmed as *S. khirikhana* TH2012^T by 16S rRNA PCR followed by amplicon sequencing analysis and chemical characteristics with API 20E biochemical strip tests (data not shown), was used to prepare inoculum for an additional immersion challenge test of 10^5 CFU ml⁻¹ in the challenge group along with an untreated control group (see Experimental Procedures). From this second challenge series to confirm Koch's postulates, the results showed that TH2012^T caused 100% mortality within 141 hpi. The same unique histopathological lesions were observed for both this and the first series of bacterial challenge tests (see below).

Clinical signs of TH2012^T challenged shrimp

Similar to AHPND diseased shrimp (Lightner *et al.*, 2012; Naca, 2012; Tran *et al.*, 2013), TH2012^T-infected shrimp showed lethargy and swimming in a slow movement or in a spiral direction. Unlike AHPND diseased shrimp, TH2012^T-infected shrimp had visibly white abdominal muscle but did not show other clinical signs of AHPND such as empty or interrupted gut contents, pale-to-white hepatopancreata (HP) and significant atrophy of HP.

TH2012^T kills shrimp with unique histopathology but no pathognomonic AHPND lesions

Altogether, 40 shrimp were examined from three challenge experiments carried out independently with separate sources of shrimp. Shrimp examined in the first two challenge experiments (total 15 each) included three control shrimp and 12 moribund shrimp (four each from immersion challenges at 10^4 to 10^6 CFU ml⁻¹), whereas in the third experiment (total 10 shrimp), three control shrimp and seven moribund shrimp (three each from immersion challenges 10^4 and 10^5 CFU ml⁻¹ and only one from immersion challenge 10^6 since all others from that group had died before they could be retrieved for fixation while still alive).

From the three challenge experiments, none of the shrimp in the control (total nine examined) or in the immersion challenge groups (total 31 examined) showed the pathognomonic lesions of acute AHPND characterized by massive sloughing of the HP tubular epithelial cells (Lightner *et al.*, 2012; Naca, 2012; Tran *et al.*,

2013). The most consistent and prominent histopathological abnormality in the moribund shrimp challenged by immersion exposure to TH2012^T were bacteria-free lesions in the ventral nerve cord that were absent in all nine control shrimp examined. These lesions consisted of abnormal nerve cord nuclei distorted in the two-dimensional sections into variable shapes somewhat resembling jigsaw puzzle pieces ('jigsaw-piece nuclei' or JPN) (Fig. 2A–E) and/or highly vacuolated ('foamy') cytoplasm in the giant nerve cells (FGC) of associated nerve ganglia (Fig. 3). Out of the 31 moribund shrimp tissue sections examined, two did not include ventral nerve cord tissue, but all of the remaining 29 (100%) showed JPN and/or FGC. We propose this previously unreported feature of JPN to be used as a strong presumptive indicator pathognomonic for disease caused by *S. khirikhana*. Inspection of JPN with the oil emersion lens suggested

that the misshapen nuclei were caused by pressure from cytoplasmic vacuoles (Fig. 2F). Whether or not any of these vacuoles are intra-nuclear would need to be resolved by using transmission electron microscopy. The histological features described above could be clearly visualized using a light microscope with a 40x objective. They indicated a severe negative response to *S. khirikhana* challenge in the shrimp nervous system, and the absence of bacterial cells in the lesions suggested the possibility that this response involved a causal neurotoxin.

The next most consistent lesion in the 31 moribund shrimp (absent in the control shrimp and also clearly visualized using a light microscope with a 40x objective) was the abnormal presence of cytoplasmic vacuoles in the tubule matrix cells of the lymphoid organ (LO) with bacteria absent for 25/26 (96%) of the specimens with

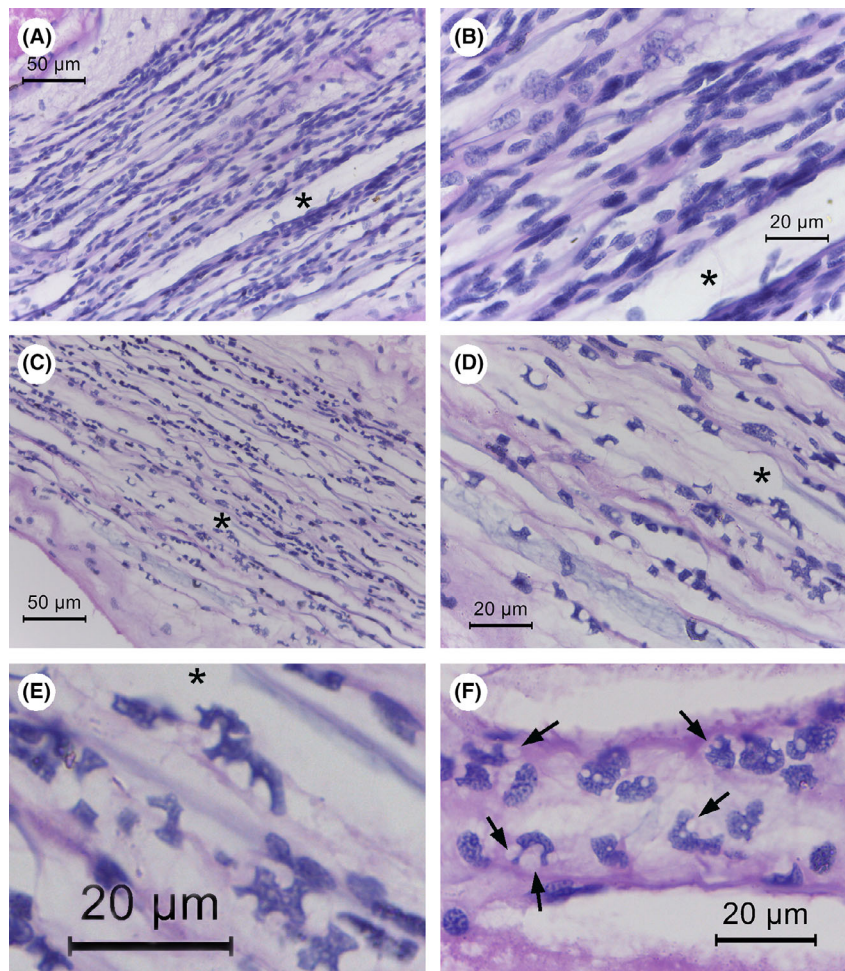


Fig. 2. Photomicrographs of ventral nerve cord histology of normal and moribund shrimp from *S. khirikhana* TH2012^T challenge tests. Asterisks (*) indicate the same location in photomicrographs at different magnifications. A and B. A control shrimp showing normal nerve cord histology at low and high magnification respectively. C, D and E. Moribund shrimp histopathology at progressively higher magnifications showing irregularly shaped nuclei reminiscent of scattered jigsaw puzzle pieces (JPN). F. Example of JPN in a section where pressure from adjacent vacuoles appears to be the cause of their abnormal shapes (arrows).

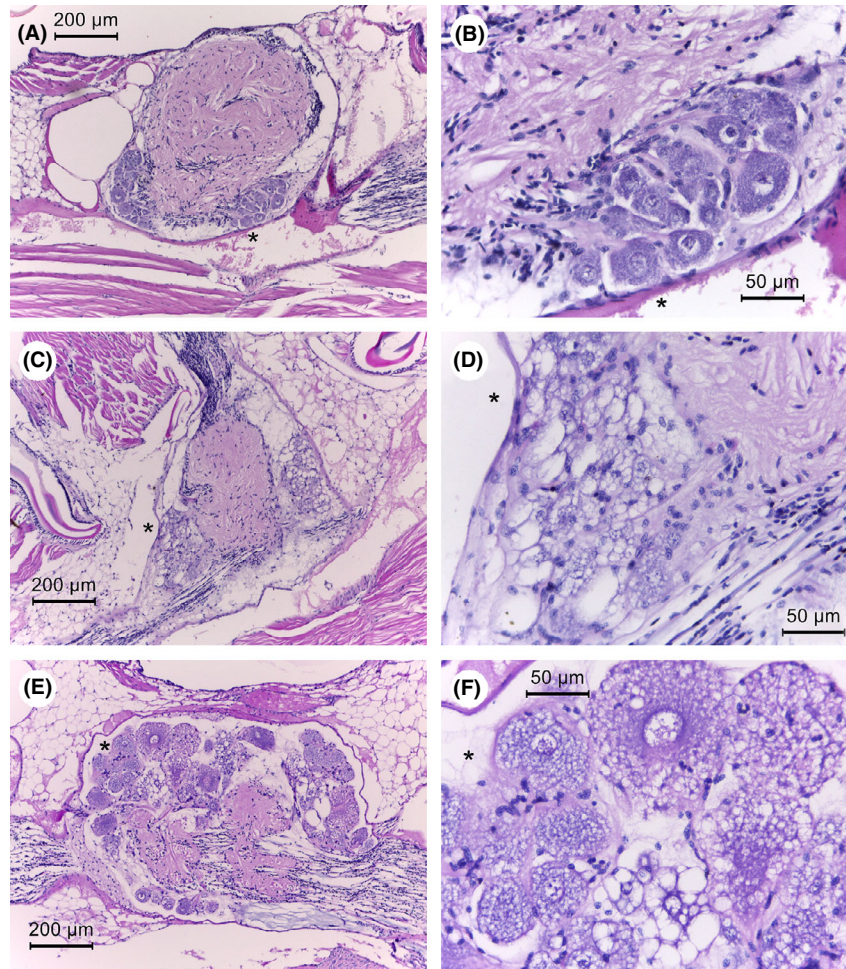


Fig. 3. Photomicrographs of ventral nerve cord ganglia of normal and moribund shrimp from *S. khirikhana* TH2012^T challenge tests. Asterisks (*) indicate the same location in photomicrographs at different magnifications. A and B. A control shrimp showing normal nerve cord histology at low and high magnification, respectively. C–F. Moribund shrimp histopathology at progressively higher magnifications showing highly vacuolated cytoplasm of giant nerve cells.

LO tissue in their sections (Fig. 4). This gave rise to a marked decrease in the normal nuclear density of the LO tubule matrices that was clearly visible using a light microscope with a 40x objective. Many of these vacuoles contained eosinophilic inclusions of variable shape but smaller than the adjacent nuclei. In most cases, the interstitial spaces between the tubules also contained abnormal vacuoles with eosinophilic inclusions. Also, in some specimens these features were accompanied by scattered pyknotic and karyorrhectic nuclei (8/27 specimens). All seven control shrimp sections that included LO (i.e. two sections without LO) showed normal LO histology (Fig. 4). For the two moribund shrimp specimens whose sections lacked nervous tissue (see above) both contained LO tissue that showed LO lesions. Thus, combined examination of both the nervous and LO tissues for lesions was sufficient to yield a positive presumptive diagnosis result for disease caused by *S. khirikhana* in

all 31 of the moribund shrimp specimens examined. There was no indication of accompanying LO spheroid formation as is frequently reported during the shrimp response to viral and bacterial pathogens (Hasson *et al.*, 1999; Anggraeni and Owens, 2000; Van De Braak *et al.*, 2002; Owens, 2010). It is possible that the loss of LO function was prevented or too rapid to allow for spheroid formation.

Additional, but less ubiquitous distinctive histological abnormalities presented in the moribund shrimp but absent in the control shrimp are described in Supporting information. These included the digestive system with unusual vacuolization of (i) the anterior midgut caecum (AMC) (22/26 = 85% of specimens with AMC tissue in the section; Fig. S13), of (ii) nearby subcuticular epithelial cells of the stomach (24/26 = 92% of specimens with appropriate tissue in the section; Fig. S14) and of (iii) E-cells of the tubule epithelium of the hepatopancreas (HP)

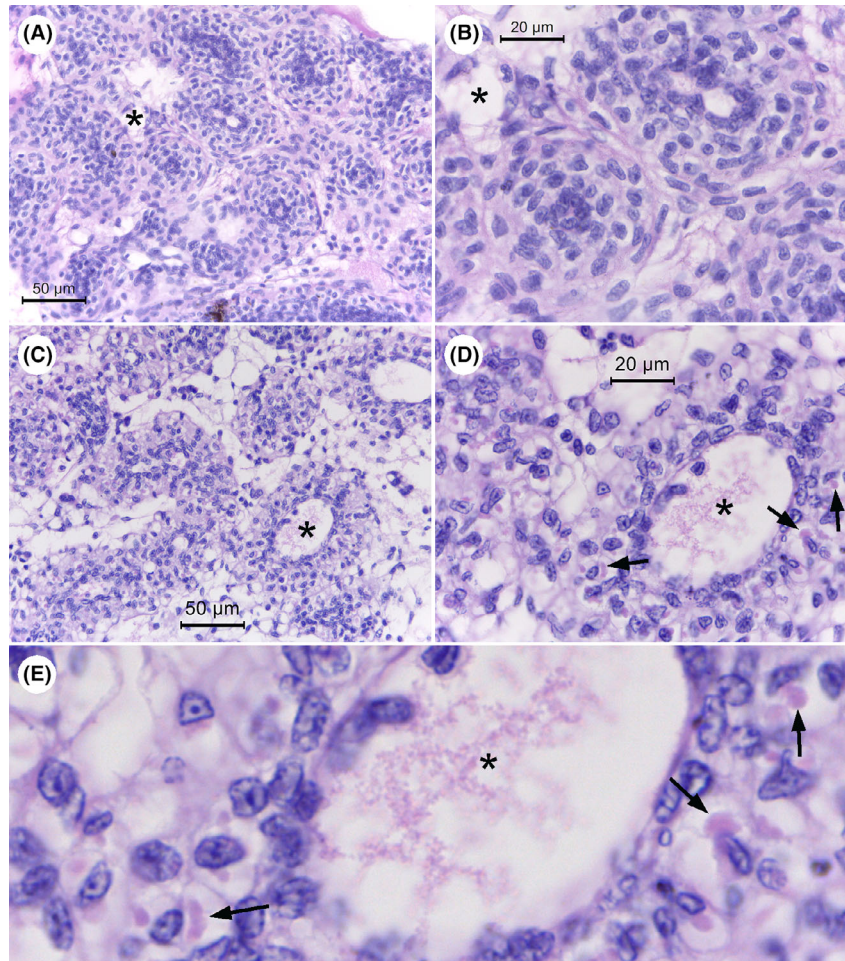


Fig. 4. Photomicrographs of histology of the lymphoid organ (LO) of normal shrimp and moribund shrimp from immersion with *S. khirikhana* TH2012^T. Asterisks (*) indicate the same location in photomicrographs at different magnifications. A and B. Example of normal LO tissue from control shrimp at low and high magnification respectively. C–E. Example of histopathology of LO tissue from test shrimp at progressively higher magnifications showing extensive cell vacuolization with some cells showing the presence of eosinophilic cytoplasmic inclusions (arrows).

(22/31 = 71% of specimens; Fig. S15). Also found were hematopoietic tissue (HT) lesions showing prominent eosinophilic, cytoplasmic inclusions (sometimes within vacuoles) (20/31 = 65% of moribund shrimp specimens examined; Fig. S16), and focal gill lesions showing pyknotic and karyorrhectic nuclei, eosinophilic cytoplasmic inclusions and loss of gill structure (25/31 = 81% of moribund shrimp; data not shown). None of these are reliable for presumptive diagnosis when compared to the nerve cell and LO lesions due to their low prevalence, excessive time needed for analysis or difficulty in detection (i.e. an 100x oil immersion lens is required for HT examination in contrast to the 40x lens sufficient for examination of nervous and LO tissues). Note that no bacterial cells were observed in the lesions described above, but that they were seen occasionally in the HP tubule lumens of moribund shrimp specimens from the bacterial challenge (11/31 = 35.5% moribund shrimp; Fig. S17).

Putative virulence factors

In the TH2012^T genome, no *Pir*^{VP} sequences of VP_{AHPND} (Han *et al.*, 2015; Lee *et al.*, 2015; Xiao *et al.*, 2017) or *Pir*^{VP}-like sequences of *S. violacea* and no significant nucleotide similarity of pSTH1 to the *Pir*^{VP} toxin carrying plasmids were found by exhaustive searches (Supporting information) (Wechprasit *et al.*, 2019). GIPSY (Soares *et al.*, 2016) reported six PAIs and two RIs in the TH2012^T genome (Fig. 5). Two PAIs gave strong prediction scores and one gave a normal score, and the others gave weak scores. The two with strong scores contained putative genes of the Type VI secretion system (T6SS) along with fimbrial and colonization factor genes, lysozyme, extracellular phospholipase, microbial serine proteinase and hypothetical proteins. There were two putative RIs, one each with strong and weak prediction score. The weak score RI was in the same region as

one of the three weak score PAIs (Fig. 5). Genes in the RIs included putative multidrug efflux pumps MacA–MacB pumps, *MarR* family genes, several permease proteins, OmpF porin, and *evgS* and *PhoP* genes. In addition, the TH2012^T genome contains a putative prophage (Fig. 5) (Wechprasit *et al.*, 2019) and some virulence genes found in some *Shewanella* isolates (Paździor, 2016; Yousfi *et al.*, 2017) such as putative

haemolysins, chitinases and proteases (Wechprasit *et al.*, 2019).

Discussion

The phylogenetic tree analysis (Fig. 1, Figs S2–S6) and DNA–DNA relatedness indicated that isolate TH2012^T represents a new species of *Shewanella*, separated from

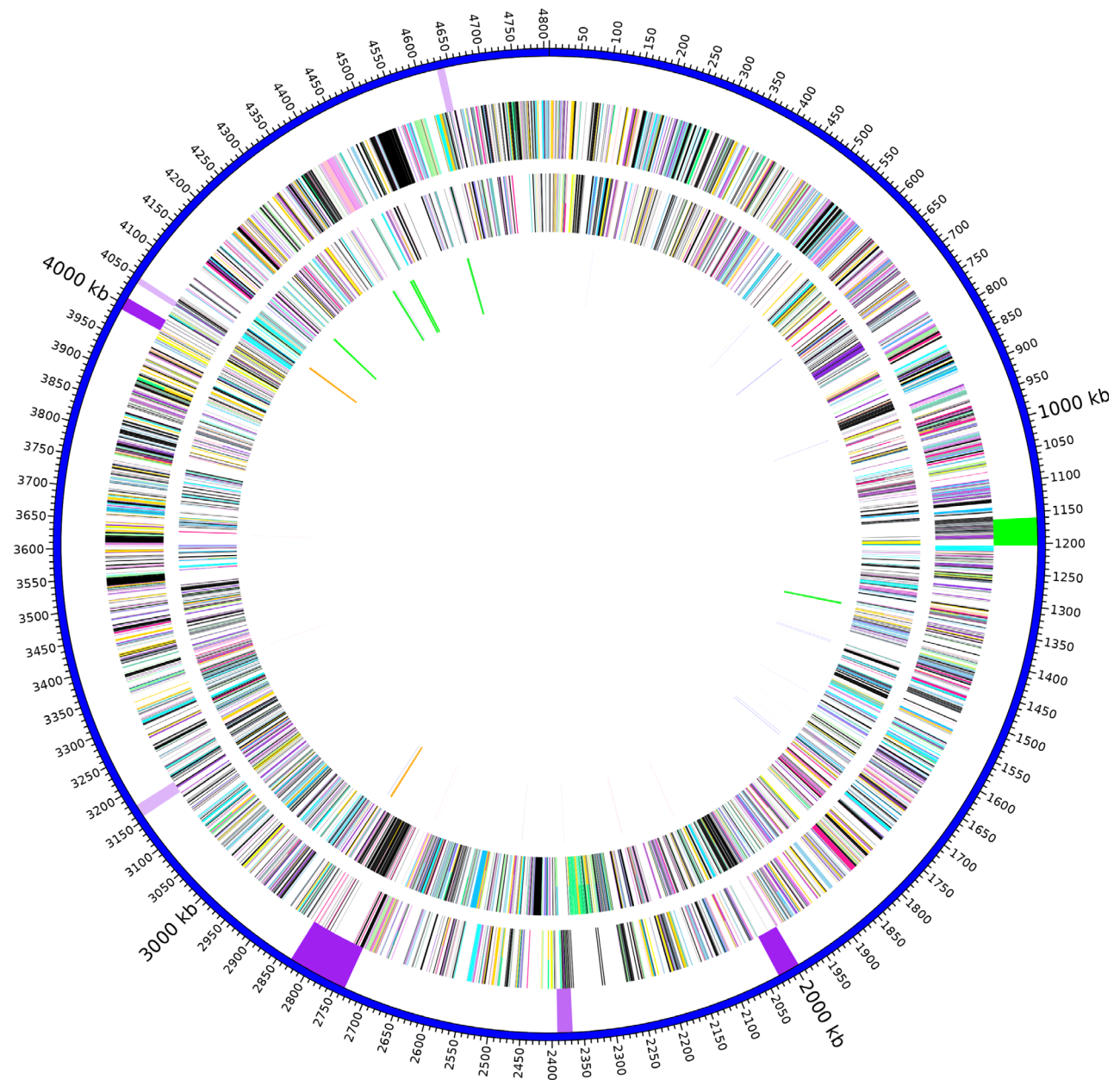


Fig. 5. Graphical map of the chromosome of *S. khirikhana* TH2012^T. From the outside to the centre: pathogenicity or resistance islands (darker purple indicates stronger prediction scores) and prophage (green), genes on the forward strand (coloured by COG categories), genes on the reverse strand (coloured by COG categories) and RNA genes (tRNAs forward strand blue, tRNAs on reverse strand pink, rRNAs on forward strand green, rRNAs on reverse strand orange and tmRNAs on forward strand tan). COG colour and functional designations are described in Table S5.

other *Shewanella* species including type strains of *S. amazonensis* and *S. litorisediminis*. This was supported by differential morphological and physiological characteristics (Table 1 and Supporting information). Recently, an independent phylogenomic analysis of our published TH2012^T genome sequence (Wechprasit *et al.*, 2019) also supported this erection of a new species within the genus (Thorell *et al.*, 2019). Thus, we propose the name *Shewanella khirikhana* to indicate that TH2012^T originated from Prachuap Khirikhan Province, Thailand. The full description of the species is given below. Our phylogenetic tree analysis also raised the question as to whether TBRC 5001 and LV 5 can be included as representatives of *S. litorisediminis* based solely on analysis of partial 16S rRNA sequences (Fig. S3). Lacking full genome sequences for the type strain of *S. litorisediminis* SMK1-12^T, for the strains of TBRC 5001 and LV 5, and for the unidentified isolate *S. sp.* AK55, similar comparisons could not be carried out to establish clear placement of TBRC 5001, LV 5 and AK55.

By satisfying Koch's postulates, we have demonstrated that *S. khirikhana* TH2012^T is lethal to shrimp (60-h LC₅₀ ~ 10⁵ CFU ml⁻¹) and is the first from its genus to constitute an emerging shrimp pathogen. Its origin from moribund shrimp in an EMS/AHPND outbreak pond lends some support to the hypothesis that it could possibly cause some of the unexplained mortality in EMS ponds (Sanguanrut *et al.*, 2018) or even in other non-EMS ponds with unexplained mortality. In addition, it is possible that it might act together with AHPND bacteria in an additive or synergistic way to exacerbate shrimp mortality as earlier hypothesized (FAO, 2013). However, these speculations need to be confirmed or dismissed via subsequent comparison of results from single and co-challenge tests in the laboratory. For such work, the molecular tools described herein will be useful.

So far, within the genus *Shewanella*, the species *S. algae* and *S. putrefaciens* have been reported as the two major species infecting humans (e.g. septicaemia, cellulitis, arthritis, otitis and pneumonia). Both are often recovered from mixed microbial flora of patients (Satomi, 2013; Yousfi *et al.*, 2017). They have also been reported to be opportunistic pathogens in aquatic species. For example, *S. algae* caused abalone mortalities in China and Taiwan (Cai *et al.*, 2006) and ulcer disease in marine channel bass in China ((Chen *et al.*, 2003) in (Cai *et al.*, 2006)). *S. putrefaciens* has been reported from several counties as a marine and freshwater fish pathogen for tilapia, European sea bass, rabbitfish, loach, siberian sturgeon, hybrid sturgeon, rainbow trout and carp. Recently, outbreaks have been reported in farmed freshwater fish in Poland (for review see (Paździor, 2016)). It also caused mortality in freshwater zebra

mussels in North America (Gu and Mitchell, 2002). In China, *S. marisflavi* caused high mortality in sea cucumbers (Li *et al.*, 2010), and *S. aquimarina* was associated with a lesion syndrome of sea urchin (Wang *et al.*, 2013). In shrimp, *Shewanella* species, and especially *S. putrefaciens* and *S. baltica*, were associated with spoilage of *P. vannamei* stored at low temperature (Qian *et al.*, 2013; Qian *et al.*, 2015; Zhu *et al.*, 2017), and *Shewanella* species were also found to be a normal part of the bacterial flora in the *P. vannamei* gut (Suo *et al.*, 2017).

Histopathology caused by *S. khirikhana* TH2012^T in infected shrimp was unique (Figs 2–4, Figs S13–S17) and did not show the pathognomonic lesions of acute AHPND (Lightner *et al.*, 2012; Naca, 2012; Tran *et al.*, 2013). Based on prevalence, unique character and ease of examination using a 40x objective with a light microscope, we recommend that histological analysis of shrimp suspected of exposure to *S. khirikhana* focus initially on the tissue of the ventral nerve cord and the LO in standard, mid-longitudinal cephalothorax sections. This would allow for presumptive diagnosis based on the distinctive histopathology for the nerve cord (Figs 2 and 3) and the LO (Fig. 4). The other histopathological lesions described in Supporting information can be used as backups, if by chance the nerve cord and the LO are absent in a tissue section. However, this is unlikely since it is usually recommended to examine at least 10 shrimp specimens from a disease outbreak pond and it is usual by these standard procedures (Bell and Lightner, 1988) that most tissue sections would include both the ventral nerve cord and the LO, rarely only one or the other and very rarely neither.

We further recommend that any presumptive diagnosis should be confirmed by PCR testing for *S. khirikhana* followed by sequencing of any PCR amplicons. This would be facilitated since tests of EMS shrimp for AHPND bacteria involves an enrichment step that would probably also enrich for *S. khirikhana* such that the same DNA extract could be used to test for both pathogens. This would help in determining prevalence of *S. khirikhana* in EMS outbreak ponds and also indicate whether there is any positive association between occurrence of *S. khirikhana* and AHPND. We would welcome cooperation with anyone who is testing for AHPND bacteria using DNA extracts but does not or cannot test for *S. khirikhana* (see Supporting information for our free sample testing).

The nerve cord, LO and other distinctive tissue pathological lesions described here for *S. khirikhana* showed no visible bacterial cells, and since free, rod-shaped bacterial cells were seen in hepatopancreatic tubule lumens only occasionally (11/31 = 35.5%; see Supporting information). Thus, the overall results for the *S. khirikhana*

immersion challenges were similar to those for the acute phase of AHPND where bacterial cells are absent in the HP lesions at acute stage of disease. This suggests, like AHPND, that the cause of the unique histological changes in the moribund shrimp from our immersion challenge was one or more toxic substances produced by *S. khirikhana* located in the immersion water or in the shrimp stomach.

The fact that *S. khirikhana* often causes distinctive histopathological lesions (i.e. vacuolization in the E-cells of the HP) indicates that it targets, at least in part, in the same organ that is the main target of the Pir^{VP} toxins of AHPND-causing bacteria. Because of this, it is possible that mixed infections of *S. khirikhana* with AHPND bacteria could interact in an additive or synergistic manner such that normally non-lethal concentrations for each would become lethal when combined. The prospect of a synergistic increase in virulence in mixed infections is of particular concern and should be further investigated.

Absence of Pir^{VP} (VP_{AHPND}) and Pir^{VP}-like (*S. violacea*) homologous sequences in the genome of TH2012^T (Wechprasit *et al.*, 2019) suggests that one or more of other putative toxins or virulence factors may be involved in its pathogenesis. Information on virulence factors in the genus *Shewanella* is still limited. In humans, a higher virulence for *S. algae* than for *S. putrefaciens* was found to be associated with the production of beta-haemolysin and other extracellular enzymes (Khashe and Michael Janda, 1998; Yousfi *et al.*, 2017). Genomic analysis of *S. algae* MARs 14 (a multidrug-resistant pneumonia agent) revealed putative virulence factors, including haemolysin and flagellum system genes along with drug-resistance genes and multidrug efflux pump genes (Cimmino *et al.*, 2016).

Six putative PAIs and two putative RIs were detected in TH2012^T (Fig. 5). T6SS is known to play an important role in pathogenesis and bacterial competition by translocating toxic effector proteins into hosts or other bacterial cells (e.g. Jani and Cotter, 2010; Russell *et al.*, 2014)). EvgS is a member of the two-component regulatory system EvgS/EvgA, and PhoP is a member of another two-component system PhoPQ. These two systems are known to be involved in regulation of expression of the AcrAB-TolC efflux system of *E. coli* (for review see (Li *et al.*, 2015)). The MarR family genes are known to be involved in a regulatory cascade that decreases OmpF porin expression, resulting in decreased drug uptake, which in turn leads to drug resistance (see (Fernández and Hancock, 2012; Li *et al.*, 2015)). Interestingly, many transposases (24 ORFs out of the total 78 ORFs) were found scattering in one PAI, suggesting that genes in this region might be strongly linked with mobile genetic elements. Along with a prophage, other virulence genes in some *Shewanella* isolates

(Paździor, 2016; Yousfi *et al.*, 2017) such as haemolysins, chitinases and proteases are also present in the TH2012^T genome (Wechprasit *et al.*, 2019).

In summary, we have described a new bacterial species *Shewanella khirikhana* sp. nov. TH2012^T isolated from the hepatopancreas of a shrimp specimen taken from a cultivation pond experiencing an outbreak of EMS/AHPND. It is distinct from its currently known closest phylogenetic sister species *S. amazonensis* and *S. litorisediminis*. We have shown that *S. khirikhana* TH2012^T is lethal to shrimp and causes distinctive histopathology that differs markedly from the pathognomonic lesions of AHPND. It can be used as a preliminary, presumptive diagnosis for infection with *S. khirikhana*. In addition, it harbours several virulence factors in putative pathogenicity and resistance islands. However, its impact on shrimp production in terms of a direct or potentiating cause of mortality remains to be determined. The complete genome sequence of TH2012^T is a ready source for the development of a highly sensitive and specific detection method to study the prevalence of *S. khirikhana* in order to determine its full impact on shrimp culture and to control its spread.

Description of *Shewanella khirikhana* sp. nov

The specific epithet in the name *Shewanella khirikhana* (khi.ri.khan.a, adj. *khirikhana*) refers to its origin from a shrimp pond in Prachuap Khirikhan Province, Thailand, where the shrimp samples were collected for isolation of the type strain.

Cells are facultative anaerobic, free-living, Gram-negative, straight rods and motile. Colonies are yellowish, translucent, circular, smooth and convex with entire edges. Cultures grow at 25–37°C over the salinity range of 0.5–5.5% (w/v) NaCl and over the pH range 6.5–9 with optimal growth at 30 °C, pH 7–7.5 and 1.5–2% NaCl. Cultures die at 4°C and so should not be stocked in a refrigerator. However, they can be stored using standard methods at –80°C with cryoprotectant. TH2012^T produces H₂S, shows oxidase activity and can reduce nitrate to nitrite, hydrolyse Tween 20, gelatin and casein but not urea, and it does not ferment glucose and citrate, and does not show ornithine decarboxylase, beta-galactosidase, arginine dihydrolase, lysine decarboxylase and tryptophan deaminase activities. D-glucose, D-mannitol, inositol, D-sorbitol, L-rhamnose, D-melibiose, amygdalin, citrate, L-arabinose and D-sucrose are not utilized as carbon source. Production of indole and acetoin is absent.

The sequenced genome of the type strain TH2012^T has a G + C content of 54.88%, is 4.85 megabase pairs (Mbp) in size and contains a single circular chromosome (4.80 Mbp) and a circular plasmid pSTH1 (0.05 Mbp). The sequences of 16S rRNA, atpA (ATP synthase F1 subunit

alpha), mreB (rod shape-determining protein) and rpoA (DNA directed RNA polymerase subunit alpha) genes of the type strain TH2012^T are deposited under the GenBank/EMBL/DDBJ accession numbers MH719102, MH719105, MH705614, MH705617 and MH705620 respectively. The complete genome sequence of the type strain TH2012^T has also been deposited at GenBank/EMBL/DDBJ under the accession number CP020373 and at DOE JGI Integrated Microbial Genomes & Microbiomes under GOLD ID Gp0206473. Strain TH2012^T is the type strain of *Shewanella khirikhana* sp. nov. and has been deposited as TBRC 8956^T and NBRC 113603^T at Thailand Bioresource Research Center and Japan Biological Resource Center, NITE respectively.

Experimental procedures

Bacterial isolates and cultures

The bacterial isolate TH2012^T was obtained during bacterial isolation from hepatopancreatic tissue of diseased shrimp from an EMS/AHPND outbreak in 2012 (Joshi *et al.*, 2014) and was identified as a putative member of the genus *Shewanella* (Wechprasit *et al.*, 2019). Two other *Shewanella* isolates, *S. litoreisdiminis* KCTC 23961^T (= SMK1-12^T) and *S. litoreisdiminis* TBRC 5001, were obtained from the Korean Collection for Type Cultures (KCTC) and the Thailand Bioresource Research Center (TBRC) respectively. All isolates were revived from cryopreserved glycerol stocks by overnight culturing aerobically at 30°C in tryptic soy broth (TSB) supplemented by 1.5% (w/v) NaCl under shaking conditions before subsequent use. Note that all TSB and tryptic soy agar (TSA) used in this study were supplemented by 1.5% NaCl (resulting in a final NaCl content of 2.0%) unless otherwise indicated.

Morphological and physiological characteristic tests

The procedures to investigate cell morphology, biochemical characteristics with API®biomerieux API 20E stripe tests, enzyme activities (casein hydrolysis, lipase activity and gelatin hydrolysis), effects of temperature, salinity and pH on TH2012^T growth and its growth curve are described in Supporting information.

Shrimp immersion bioassay and histopathology

Penaeus vannamei (3–5 g) purchased from a local hatchery were maintained in 50 litre (L) aerated tanks containing 20 L artificial seawater (Marinium) at 15 ppt salinity and 30 °C. Shrimp (10) were acclimatized in each tank for 3 days. Then, they were challenged by immersion with TH2012^T at the concentrations of 10⁴, 10⁵ and 10⁶ colony-forming units per millilitre (CFU ml⁻¹)

with two replicate tanks for each concentration. Stock inoculum of TH2012^T for addition to shrimp immersion water was prepared by addition of as a starter culture from cryopreserved bacteria inoculated to achieve optical density at 600 nm (OD600) ~ 0.05 cultivation to obtain OD600 of 2.6 (~ 10⁹ CFU ml⁻¹ variable bacterial cell count; see Supporting information). Such stock inoculum was diluted in TSB such that 200 ml added to each shrimp culture tank would achieve the desired final bath-challenge bacterial concentrations in 20 L artificial sea water. Negative control groups were two tanks without any treatment. For 102 h post immersion (hpi), moribund and dead shrimp were recorded to determine the 50% lethal concentration at 60 hpi. Whole moribund shrimp and normal control shrimp were fixed in Davidson's fixative for histopathological analysis according to Bell and Lightner (Bell and Lightner, 1988) (see Supporting information). Similarly, the subsequent bacterial immersion challenge carried out to satisfy Koch's postulates used TH2012^T re-isolated from a moribund shrimp at 10⁵ CFU ml⁻¹ with 1–2 g shrimp.

Phylogenetic analysis by multilocus sequence analysis and genome comparison

Sequences of 16S rRNA, atpA (ATP synthase F1 subunit alpha), mreB (rod shape-determining protein) and rpoA (DNA directed RNA polymerase subunit alpha) genes of TH2012^T were obtained from the TH2012^T genome assembly (Wechprasit *et al.*, 2019), and these genes were previously used for phylogenetic analysis of *Shewanella* (Dikow, 2011). The homologous sequences in *S. litoreisdiminis* SMK1-12^T and TBRC 5001 were obtained by sequencing PCR amplicons of genomic DNA template (see Supporting information). The homologous sequences in other *Shewanella* species were obtained from GenBank (<ftp://ftp.ncbi.nlm.nih.gov/genomes/all/>). Multiple sequence alignments were performed with MUSCLE (Edgar, 2004) using concatenated multilocus sequence alignment with genes in the order of 16S rRNA, atpA, mreB and rpoA genes, and phylogenetic trees were constructed with the neighbour-joining, minimum evolution, maximum-likelihood and maximum parsimonious algorithms (all with Jukes–Cantor distance) in MEGA 7 (Kumar *et al.*, 2016). Complete genomes of TH2012^T (Wechprasit *et al.*, 2019) and *S. amazonensis* SB2B^T (Accession: NC_008700) were used to calculate digital DNA:DNA hybridization (dDDH) similarities by the Genome-to-Genome Distance Calculator version 2.1 formula 2 (<http://ggdc.dsmz.de> (Meier-Kolthoff *et al.*, 2013)) as well as to calculate average nucleotide identity (ANI) scores in IMG/MER (Chen *et al.*, 2017). GIPSY (Soares *et al.*, 2016) was used to detect pathogenicity islands and resistance islands by using the genome sequence of

TH2012^T as a query against the whole genome sequence of *S. amazonensis* SB2B^T (NC_008700) as a reference.

Acknowledgements

We would like to thank N. Munkongwongsiri, R. Suebsing, P. Sanguanrut and W. Eamsaard for their help in laboratory, BIOTEC's Biostatistics & Informatics Laboratory, and Aung T.R.H. and K. Anekthanakul for their programming and HPC support. This work was supported by the Agricultural Research Development Agency (ARDA) (grant number 8669), Mahidol University and the National Center for Genetic Engineering and Biotechnology (BIOTEC) of the National Science and Technology Development Agency (NSTDA). PW also would like to acknowledge the support from Thailand Graduate Institute of Science and Technology Scholarship (TGIST grant number SCA-CO-2560-4497-TH).

Conflict of interest

None declared.

References

Anggraeni, M.S., and Owens, L. (2000) The haemocytic origin of lymphoid organ spheroid cells in the penaeid prawn *Penaeus monodon*. *Dis Aquat Organ* **40**: 85–92.

Bell, T. A., and Lightner, D. V. (1988) *A Handbook of Normal Penaeid Shrimp Histology*. Baton Rouge, LO: World Aquaculture Society.

Cai, J., Chen, H., Thompson, K.D., and Li, C. (2006) Isolation and identification of *Shewanella* alga and its pathogenic effects on post-larvae of abalone *Haliotis diversicolor supertexta*. *J Fish Dis* **29**: 505–508.

Chen, C., Hu, C.Q., Chen, X.Y., and Zhang, L.P. (2003) Identification and characterization of *Shewanella* alga as a novel pathogen of ulcer disease of fish *Scinenops ocellata*. *Oceanologia et Limnologia Sinica* **34**: 2–8.

Chen, I.-M.A., Markowitz, V.M., Chu, K., Palaniappan, K., Szeto, E., Pillay, M., *et al.* (2017) IMG/M: integrated genome and metagenome comparative data analysis system. *Nucleic Acids Res* **45**: D507–D516.

Cimmino, T., Olaitan, A.O., and Rolain, J.-M. (2016) Whole genome sequence to decipher the resistome of *Shewanella* algae, a multidrug-resistant bacterium responsible for pneumonia, Marseille, France. *Expert Rev Anti Infect Ther* **14**: 269–275.

De La Peña, L.D., Cabillon, N.A.R., Catedral, D.D., Amar, E.C., Usero, R.C., Monotilla, W.D., *et al.* (2015) Acute hepatopancreatic necrosis disease (AHPND) outbreaks in *Penaeus vannamei* and *p. monodon* cultured in the Philippines. *Dis Aquat Organ* **116**: 251–254.

Dhar, A. K., Piamsomboon, P., Aranguren, L. F., and Kanrar, S. (2018). First report of the presence of acute hepatopancreatic necrosis disease (AHPND) in Texas, USA. URL <https://www.was.org/meetings/ShowAbstract.aspx?Id=75594>

Dikow, R.B. (2011) Genome-level homology and phylogeny of *Shewanella* (Gammaproteobacteria: Iteromonadales: Shewanellaceae). *BMC Genom* **12**: 237.

Edgar, R.C. (2004) MUSCLE: multiple sequence alignment with high accuracy and high throughput. *Nucleic Acids Res* **32**: 1792–1797.

FAO (2013) FAO Report of the FAO/MARD technical workshop on early mortality syndrome (EMS) or acute hepatopancreatic necrosis syndrome (AHPNS) of cultured Shrimp (under TCP/VIE/3304), Hanoi, Viet Nam on 25–27 June 2013. Rome, p. 55.

Fernández, L., and Hancock, R.E.W. (2012) Adaptive and mutational resistance: role of porins and efflux pumps in drug resistance. *Clin Microbiol Rev* **25**: 661–681.

Goris, J., Konstantinidis, K.T., Klappenbach, J.A., Coenye, T., Vandamme, P., and Tiedje, J.M. (2007) DNA-DNA hybridization values and their relationship to whole-genome sequence similarities. *Int J Syst Evol Microbiol* **57**: 81–91.

Gu, J.-D., and Mitchell, R. (2002) Indigenous microflora and opportunistic pathogens of the freshwater zebra mussel, *Dreissena polymorpha*. *Hydrobiologia* **474**: 81–90.

Han, J.E., Tang, K.F.J., Tran, L.H., and Lightner, D.V. (2015) Phototransducing insect-related (Pir) toxin-like genes in a plasmid of *Vibrio parahaemolyticus*, the causative agent of acute hepatopancreatic necrosis disease (AHPND) of shrimp. *Dis Aquat Organ* **113**: 33–40.

Han, J.E., Tang, K.F.J., Aranguren, L.F., and Piamsomboon, P. (2017) Characterization and pathogenicity of acute hepatopancreatic necrosis disease natural mutants, pir-ABvp(-) *V. parahaemolyticus*, and pirABvp(+) *V. campbellii* strains. *Aquaculture* **470**: 84–90.

Hasson, K.W., Lightner, D.V., Mohny, L.L., Redman, R.M., and White, B.M. (1999) Role of lymphoid organ spheroids in chronic Taura syndrome virus (TSV) infections in *Penaeus vannamei*. *Dis Aquat Organ* **38**: 93–105.

Jani, A. , and Cotter, P.A. (2010) Type VI Secretion: not just for pathogenesis anymore. *Cell Host Microbe* **8**: 2–6.

Joshi, J., Srisala, J., Truong, V.H., Chen, I.-T., Nuangsaeng, B., Suthienkul, O., *et al.* (2014) Variation in *Vibrio parahaemolyticus* isolates from a single Thai shrimp farm experiencing an outbreak of acute hepatopancreatic necrosis disease (AHPND). *Aquaculture* **428–429**: 297–302.

Khashe, S., and Michael Janda, J. (1998) Biochemical and pathogenic properties of *Shewanella* alga and *Shewanella putrefaciens*. *J Clin Microbiol* **36**: 783–787.

Kondo, H., Van, P.T., Dang, L.T., and Hirono, I. (2015) Draft genome sequence of non-*Vibrio parahaemolyticus* acute hepatopancreatic necrosis disease strain KC13.17.5, isolated from diseased shrimp in Vietnam. *Genome Announcements* **3**: e00978-15.

Kumar, S., Stecher, G., and Tamura, K. (2016) MEGA7: molecular evolutionary genetics analysis version 7.0 for bigger datasets. *Mol Biol Evol* **33**: 1870–1874.

Lai, H.-C., Ng, T.H., Ando, M., Lee, C.-T., Chen, I.-T., Chuang, J.-C., *et al.* (2015) Pathogenesis of acute hepatopancreatic necrosis disease (AHPND) in shrimp. *Fish Shellfish Immunol* **47**: 1006–1014.

Lee, M.H., and Yoon, J.H. (2012) *Shewanella litorisediminis* sp. nov., a gammaproteobacterium isolated from a tidal flat sediment. *Antonie Van Leeuwenhoek* **102**: 591–599.

- Lee, C.-T., Chen, I.-T., Yang, Y.-T., Ko, T.-P., Huang, Y.-T., Huang, J.-Y., *et al.* (2015) The opportunistic marine pathogen *Vibrio parahaemolyticus* becomes virulent by acquiring a plasmid that expresses a deadly toxin. *Proc Natl Acad Sci USA* **112**: 10798–10803.
- Li, H., Qiao, G., Gu, J.-Q., Zhou, W., Li, Q., Woo, S.-H., *et al.* (2010) Phenotypic and genetic characterization of bacteria isolated from diseased cultured sea cucumber *Apostichopus japonicus* in northeastern China. *Dis Aquat Organ* **91**: 223–235.
- Li, X.-Z., Plésiat, P., and Nikaido, H. (2015) The challenge of efflux-mediated antibiotic resistance in Gram-negative bacteria. *Clin Microbiol Rev* **28**: 337–418.
- Lightner, D.V., Redman, R., Pantoja, C., Noble, B., and Tran, L. (2012) Early mortality syndrome affects shrimp in Asia. *Glob Aquacult Advocate* **15**: 40.
- Liu, L., Xiao, J., Xia, X., Pan, Y., Yan, S., and Wang, Y. (2015) Draft genome sequence of *Vibrio owensii* strain SH-14, which causes shrimp acute hepatopancreatic necrosis disease. *Genome Announcements* **3**: e01395-15.
- Meier-Kolthoff, J.P., Auch, A.F., Klenk, H.-P., and Göker, M. (2013) Genome sequence-based species delimitation with confidence intervals and improved distance functions. *BMC Bioinformatics* **14**: 60.
- Naca (2012) Report of the Asia Pacific Emergency Regional Consultation on the Emerging Shrimp Disease: Early Mortality Syndrome (EMS)/acute Hepatopancreatic Necrosis Syndrome (AHPNS). Asia Pacific Emergency Regional Consultation on the Emerging Shrimp Disease: Early Mortality Syndrome (EMS)/Acute Hepatopancreatic Necrosis Syndrome (AHPNS).
- Nunan, L., Lightner, D., Pantoja, C., and Gomez-Jimenez, S. (2014) Detection of acute hepatopancreatic necrosis disease (AHPND) in Mexico. *Dis Aquat Organ* **111**: 81–86.
- Owens, L. (2010) Insight into the lymphoid organ of penaeid prawns: a review. *Fish Shellfish Immunol* **29**: 367–377.
- Paździor, E. (2016) *Shewanella putrefaciens* - A new opportunistic pathogen of freshwater fish. *J Vet Res (Poland)* **60**: 429–434.
- Prachumwat, A., Thitamadee, S., Sriurairatana, S., Chuchird, N., Limsuwan, C., Jantratit, W., *et al.* (2012) Shotgun sequencing of bacteria from AHPNS, a new shrimp disease threat for Thailand. Poster. URL <http://library.enaca.org/Health/DiseaseLibrary/ahpns-poster-nru-summit.pptx>
- Prachumwat, A., Taengchaiyaphum, S., Mungkongwongsiri, N., Aldama-Cano, D.J., Flegel, T.W., and Sritunyalucksana, K. (2019) Update on early mortality syndrome/acute hepatopancreatic necrosis disease by April 2018. *J World Aquaculture Soc* **50**: 5–17.
- Qian, Y.-F., Xie, J., Yang, S.-P., and Xiong, Q. (2013) Study of the microbiota in Pacific white shrimp (*Litopenaeus vannamei*) under varying O₂ modified atmosphere packaging using PCR-DGGE. *J Pure Appl Microbi* **7**: 87–93.
- Qian, Y., Yang, S., Xie, J., Wu, W., Xiong, Q., and Gao, Z. (2015) Studies on the putrefaction potential of the specific spoilage organisms from modified atmosphere packaged *Litopenaeus vannamei*. *J Chin Institute Food Sci Technol* **15**: 85–91.
- Russell, A.B., Peterson, S.B., and Mougous, J.D. (2014) Type VI secretion system effectors: poisons with a purpose. *Nat Rev Microbiol* **12**: 137–148.
- Sanguanrut, P., Mungkongwongsiri, N., Kongkumnerd, J., Thawonsuwan, J., Thitamadee, S., Boonyawiwat, V., *et al.* (2018) A cohort study of 196 Thai shrimp ponds reveals a complex etiology for early mortality syndrome (EMS). *Aquaculture* **493**: 26–36.
- Satomi, M. (2013) The family shewanellaceae. *The Prokaryotes: Gammaproteobacteria*: 597–625.
- Sirikharin, R., Taengchaiyaphum, S., Sanguanrut, P., Chi, T.D., Mavichak, R., Proespraiwong, P., *et al.* (2015) Characterization and PCR detection of binary, pir-like toxins from *Vibrio parahaemolyticus* isolates that cause acute hepatopancreatic necrosis disease (AHPND) in shrimp. *PLoS ONE* **10**: e0126987.
- Soares, S.C., Geyik, H., Ramos, R.T.J., de Sá, P.H.C.G., Barbosa, E.G.V., Baumbach, J., *et al.* (2016) GIPSy: genomic island prediction software. *J Biotechnol* **232**: 2–11.
- Suo, Y., Li, E., Li, T., Jia, Y., Qin, J. G., Gu, Z., and Chen, L. (2017) Response of gut health and microbiota to sulfide exposure in Pacific white shrimp *Litopenaeus vannamei*. *Fish Shellfish Immunol* **63**: 87–96.
- Thitamadee, S., Prachumwat, A., Srisala, J., Jaroenlak, P., Salachan, P.V., Sritunyalucksana, K., *et al.* (2016) Review of current disease threats for cultivated penaeid shrimp in Asia. *Aquaculture* **452**: 69–87.
- Thorell, K., Meier-Kolthoff, J.P., Sjöling, Å., and Martín-Rodríguez, A.J. (2019) Whole-genome sequencing redefines *Shewanella* taxonomy. *Front Microbiol* **10**: 1861.
- Tinwongger, S., Nochiri, Y., Thawonsuwan, J., Nozaki, R., Kondo, H., Awasthi, S.P., *et al.* (2016) Virulence of acute hepatopancreatic necrosis disease PirAB-like relies on secreted proteins not on gene copy number. *J Appl Microbiol* **121**: 1755–1765.
- Tran, L., Nunan, L., Redman, R.M., Mohney, L.L., Pantoja, C.R., Fitzsimmons, K., and Lightner, D.V. (2013) Determination of the infectious nature of the agent of acute hepatopancreatic necrosis syndrome affecting penaeid shrimp. *Dis Aquat Organ* **105**: 45–55.
- Van De Braak, C.B., Botterblom, M.H.A., Taverne, N., Van Muiswinkel, W.B., Rombout, J.H.W.M., and Van Der Knaap, W.P.W. (2002) The roles of haemocytes and the lymphoid organ in the clearance of injected *Vibrio* bacteria in *Penaeus monodon* shrimp. *Fish Shellfish Immunol* **13**: 293–309.
- Venkateswaran, K., Dollhopf, M.E., Aller, R., Stackebrandt, E., and Neelson, K.H. (1998) *Shewanella amazonensis* sp. nov., a novel metal-reducing facultative anaerobe from Amazonian shelf muds. *Int J Syst Bacteriol* **48** (Pt 3): 965–972.
- Wang, Y., Feng, N., Li, Q., Ding, J., Zhan, Y., and Chang, Y. (2013) Isolation and characterization of bacteria associated with a syndrome disease of sea urchin *Strongylocentrotus intermedius* in North China. *Aquac Res* **44**: 691–700.
- Wangman, P., Longyant, S., Taengchaiyaphum, S., Senapin, S., Sithigomgul, P., and Chaivisuthangkura, P. (2018) PirA & B toxins discovered in archived shrimp pathogenic *Vibrio campbellii* isolated long before EMS/AHPND outbreaks. *Aquaculture* **497**: 494–502.
- Wechprasit, P., Panphloi, M., Thitamadee, S., Sritunyalucksana, K., and Prachumwat, A. (2019) Complete genome sequence of *Shewanella* sp. strain TH2012, isolated from shrimp in a cultivation pond exhibiting early mortality syndrome. *Microbiol Resour Announc* **8**: e01703–18.

World Organization for Animal Health (2016) *Event summary: Hepatopancreatitis in Prawns, Australia*. World Organization for Animal Health. URL http://www.oie.int/wahis_2/public/wahid.php/Reviewreport/Review/viewsummary?fupser=&dothis=&reportid=19665

Xiao, J., Liu, L., Ke, Y., Li, X., Liu, Y., Pan, Y., *et al.* (2017) Shrimp AHPND-causing plasmids encoding the PirAB toxins as mediated by pirAB-Tn903 are prevalent in various *Vibrio* species. *Sci Rep* **7**: 42177.

Yousfi, K., Bekal, S., Usongo, V., and Touati, A. (2017) Current trends of human infections and antibiotic resistance of the genus *Shewanella*. *Eur J Clin Microbiol Infect Dis* **36**: 1353–1362.

Zhu, S., Zhang, C., Wu, H., Jie, J., Zeng, M., Liu, Z., *et al.* (2017) Spoilage of refrigerated (4°C) *Litopenaeus vannamei*: cooperation between *Shewanella* species and contribution of cyclo-(L-Pro-L-Leu)-dependent quorum sensing. *Int J Food Sci Technol* **52**: 1517–1526.

Supporting information

Additional supporting information may be found online in the Supporting Information section at the end of the article.

Appendix S1. Supporting Information, Figs S1–S18 and Tables S1–S5.

Fig. S1. Phylogeny of 16S rDNA genes of *Shewanella khirikhana* TH2012^T and other *Shewanella* species. The neighbour-joining phylogenetic tree with Jukes-Cantor distance was based on 1452 aligned positions of 16S rDNA gene sequences. *Moritella marina* ATCC 15381 was used as an outgroup. Bootstrap values (expressed as percentages of 1000 replications) are shown at branching points. Most of the nodes were also recovered in the trees generated with the minimum evolution (Jukes-Cantor distance), maximum-likelihood (Jukes-Cantor distance) and maximum parsimonious algorithms based on the same set of sequences, except those with *Filled circles*, or *Filled squares* were not recovered in the trees of maximum parsimonious, or both maximum parsimonious and maximum-likelihood algorithms, respectively. *Scale bar* indicates estimated sequence divergence (substitutions per nucleotide position). Sequence accession numbers are shown in the parentheses after the species names.

Fig. S2. Phylogeny 16S rDNA genes of *Shewanella khirikhana* TH2012^T and other *Shewanella* species including strains LV 5 and AK55. The neighbour-joining phylogenetic tree with Jukes-Cantor distance was based on 1176 aligned positions of 16S rDNA gene sequences. *Moritella marina* ATCC 15381 was used as an outgroup. Bootstrap values (expressed as percentages of 1000 replications) are shown at branching points. Most of the nodes were also recovered in the trees generated with the minimum evolution (Jukes-Cantor distance), maximum-likelihood (Jukes-Cantor distance) and maximum parsimonious algorithms based on the same set of sequences, except those with *Filled circles*, or *Opened squares* were not recovered in the trees of maximum parsimonious, or maximum-likelihood algorithms,

respectively. *Scale bar* indicates estimated sequence divergence (substitutions per nucleotide position). Sequence accession numbers are shown in the parentheses after the species names.

Fig. S3. Phylogeny of *atpA* genes of *Shewanella khirikhana* TH2012^T and other *Shewanella* species. The neighbour-joining phylogenetic tree with Jukes-Cantor distance was based on 1262 aligned positions of *atpA* gene sequences. *Moritella marina* ATCC 15381 was used as an outgroup. Bootstrap values (expressed as percentages of 1000 replications) are shown at branching points. Most of the nodes were also recovered in the trees generated with the minimum evolution (Jukes-Cantor distance), maximum-likelihood (Jukes-Cantor distance) and maximum parsimonious algorithms based on the same set of sequences, except those with *Opened squares*, or *Filled squares* were not recovered in the trees of maximum-likelihood, or both maximum parsimonious and maximum-likelihood algorithms, respectively. *Scale bar* indicates estimated sequence divergence (substitutions per nucleotide position). Sequence accession numbers are shown in the parentheses after the species names.

Fig. S4. Phylogeneny of *mreB* genes of *Shewanella khirikhana* TH2012^T and other *Shewanella* species. The neighbour-joining phylogenetic tree with Jukes-Cantor distance was based on 785 aligned positions of *mreB* gene sequences. *Moritella marina* ATCC 15381 was used as an outgroup. Bootstrap values (expressed as percentages of 1000 replications) are shown at branching points. Most of the nodes were also recovered in the trees generated with the minimum evolution (Jukes-Cantor distance), maximum-likelihood (Jukes-Cantor distance) and maximum parsimonious algorithms based on the same set of sequences, except those with *Filled circles*, or *Filled squares* were not recovered in the trees of maximum parsimonious, or both maximum parsimonious and maximum-likelihood algorithms, respectively. *Scale bar* indicates estimated sequence divergence (substitutions per nucleotide position). Sequence accession numbers are shown in the parentheses after the species names.

Fig. S5. Phylogeny of *rpoA* genes of *Shewanella khirikhana* TH2012^T and other *Shewanella* species. The neighbour-joining phylogenetic tree with Jukes-Cantor distance was based on 789 aligned positions of *rpoA* gene sequences. *Moritella marina* ATCC 15381 was used as an outgroup. Bootstrap values (expressed as percentages of 1000 replications) are shown at branching points. Most of the nodes were also recovered in the trees generated with the minimum evolution (Jukes-Cantor distance), maximum-likelihood (Jukes-Cantor distance) and maximum parsimonious algorithms based on the same set of sequences, except those with *Filled circles*, *Opened squares*, or *Filled squares* were not recovered in the trees of maximum parsimonious, maximum-likelihood, or both maximum parsimonious and maximum-likelihood algorithms, respectively. *Scale bar* indicates estimated sequence divergence (substitutions per nucleotide position). Sequence accession numbers are shown in the parentheses after the species names.

Fig. S6. Photomicrographs of unstained cell morphology and Gram stain morphology of *Shewanella khirikhana* TH2012^T.

Fig. S7. Colony characteristics of *Shewanella khirikhana* TH2012^T from stereomicroscope (A) and light microscope (B).

Fig. S8. Graph showing time course OD600 of *Shewanella khirikhana* TH2012^T cultured at various salinities (%NaCl).

Fig. S9. Graph showing time course OD600 of *Shewanella khirikhana* TH2012^T cultured at various pH's.

Fig. S10. Growth profiles of *Shewanella khirikhana* TH2012^T measured by optical density at 600 nm (OD600).

Fig. S11. Graph showing *Shewanella khirikhana* TH2012^T viable bacterial cell counts (CFU ml⁻¹) vs. OD600 during hours 2–4 of the growth curve experiment (hours are indicated by colors) in Fig. S10. The grey area denotes the 95% confidence level interval for predictions from a linear model of log₁₀ CFU ml⁻¹ versus log₁₀ OD600. $R^2 = 0.7814$, $P = 4.902 \times 10^{-8}$.

Fig. S12. Graph showing the regression line for shrimp mortality versus bacterial concentration (log₁₀ CFU ml⁻¹) for *Shewanella khirikhana* TH2012^T immersion bioassay up to 60 h post immersion. The grey area denotes the 95% confidence level interval for predictions from a linear model. $R^2 = 0.6945$, $P = 0.03933$.

Fig. S13. Photomicrographs of histology of the anterior mid-gut cecum (AMC) of normal shrimp and moribund shrimp from immersion with *Shewanella khirikhana* TH2012^T. (A & B) Example of normal AMC tissue at low and high magnification, respectively. (C & D) Example of histopathology from a moribund test shrimp with abnormally vacuolated epithelial cells containing few eosinophilic inclusions. (E & F) Example histopathology showing vacuolated epithelial cells containing many eosinophilic inclusions.

Fig. S14. Example photomicrographs of histology of the sub-cuticular epithelium of the stomach of normal shrimp and of moribund shrimp from immersion with *Shewanella khirikhana* TH2012^T. (A & B) Normal sub-cuticular epithelial cells at low and high magnification showing relatively non-vacuolated cytoplasm. (C & D) Abnormally vacuolated sub-cuticular epithelial cells from a moribund shrimp specimen at low and high magnification. Asterisks (*) indicate the same position in the low and high magnification photomicrographs.

Fig. S15. Photomicrographs of histology of the E-cell region of the hepatopancreas of normal shrimp and moribund shrimp from immersion with *Shewanella khirikhana* TH2012^T. (A & B) Example of normal E-cells in tubular cross section at low and high magnification, respectively,

showing dense non-vacuolated cytoplasm. (C & D) Example of abnormally vacuolated E-cells in cross-section. (E & F) Similar to C and D except that the tubules are in longitudinal section. Asterisks (*) indicate the same position in the low and high magnification photomicrographs.

Fig. S16. Example photomicrographs of histology of hematopoietic tissue (HT) of normal shrimp and of moribund shrimp from immersion with *Shewanella khirikhana* TH2012^T. (A, B & C) Normal HT at progressively higher magnification showing cells that lack eosinophilic cytoplasmic inclusions. In B and C, the arrows indicate the same cell nucleus at low and high magnification. (D, E & F) Abnormal HT at progressively higher magnification showing the presence of eosinophilic cytoplasmic inclusions. The asterisks indicate the same position at different magnifications D, E and F and the arrows mark the same eosinophilic inclusion in E & F. Note that the highest magnification (100x objective) is needed for easy identification of the unique inclusions.

Fig. S17. Photomicrographs of bacterial cells seen in some of the moribund, challenged shrimp. (A) Bacterial cells of mixed size and morphology together with sloughed epithelial cells in the lumen of a hepatopancreatic (HP) tubule. (B) Few bacterial cells of uniform morphology in the lumen of an HP tubule with an intact epithelial cell layer.

Fig. S18. Graphical map of the plasmid pSTH1. From outside to the center: Genes on forward strand (colored by COG categories), Genes on reverse strand (colored by COG categories). COG color and functional designations are described in Supporting Information Table S5.

Table S1. PCR primer sequences used in this study.

Table S2. Length (bp) of *atpA*, *mreB*, and *rpoA* sequences in strains TH2012^T, TBRC 5001, SMK1-12^T, and SB2B^T, and percentage of nucleotide identities of TH2012^T to corresponding orthologous sequences in TBRC 5001, SMK1-12^T, and SB2B^T.

Table S3. *Shewanella khirikhana* TH2012^T viable bacterial cell counts (CFU ml⁻¹) from incubation experiments at various temperature (°C). UD, unable to determine due to either no colony formation or the number of colonies were not in the range of 10–300 colonies.

Table S4. *Shewanella khirikhana* TH2012^T genome project information.

Table S5. Codes, number and percentage of genes, descriptions and colors associated with general COG functional categories.